

## КРАТКИЕ СООБЩЕНИЯ

UDC 541.6:547.13:546.75

**GEOMETRIES AND PROPERTIES OF THE HETEROBIMETALLIC PHOSPHIDO-BRIDGED COMPLEX:  
 $\text{CpW}(\text{CO})_2(\mu\text{-PPh}_2)\text{Mo}(\text{CO})_5$**

J. Wang<sup>1</sup>, X. Shi<sup>1</sup>, W. Cao<sup>2</sup><sup>1</sup>Xuzhou Institute of Technology, Xuzhou, P. R. China

E-mail: whxb@pku.edu.cn

<sup>2</sup>State Key Laboratory of Chemical Engineering, Beijing University of Technology, Beijing, P. R. China

Received April, 27, 2015

Geometries and properties of the  $\text{CpW}(\text{CO})_2(\mu\text{-PPh}_2)\text{Mo}(\text{CO})_5$  complex are investigated theoretically through HF and DFT methods. Computational results reveal that the most accurate structural parameters can be predicted at the B2PLYP/SDD level of theory. AIM and NBO analyses are performed to investigate the nature of the Mo—W and the metal–carbonyl interaction in  $\text{CpW}(\text{CO})_2(\mu\text{-PPh}_2)\text{Mo}(\text{CO})_5$ . It is confirmed that there is a Mo—W bond and a semi-bridging carbonyl group in the complex. The formation of the Mo—W bond accompanies the dominant charge transfer interactions:  $\text{BD}(1)\text{Mo1—W2} \rightarrow \text{BD}^*(1)\text{Mo1—W2}$  and  $\text{BD}(2)\text{Mo1—W2} \rightarrow \text{BD}^*(2)\text{Mo1—W2}$ . The real interaction between W and the CO ligand coordinated to molybdenum explains the observed IR  $\nu(\text{CO})$  band at  $1876 \text{ cm}^{-1}$  at room temperature and  $\delta(^{13}\text{CO})$  at 218.69 ppm at 210 K.

DOI: 10.15372/JSC20160523

**Keywords:** DFT, metal–metal bond, semi-bridging carbonyl, AIM, NBO.

One special feature of the heterobimetallic phosphido-bridged complexes is the influence of the metal–metal bond on the reactivity [1]. The dative metal–metal bond functions as a switch to control the reaction in order to obtain the desired complex. This behavior provides not only an empty site for further ligand coordination to the binuclear complex when the metal–metal bond opens but also a driving force for a further reaction when the metal–metal bond reforms. Such directional opening of the dative metal–metal bond was demonstrated by the addition of a Lewis base to the heterobimetallic phosphido-bridged and arsino-bridged complexes [2]. This property can also be considered as a cooperative effect of two adjacent metals in the binuclear complex. Thus, the heterobimetallic complexes find application in catalysis, automobile and petroleum industries, e.g. to transform hydrocarbons, to manufacture nitric acid, to convert carbon monoxide, hydrocarbons, and nitrogen oxides simultaneously in automobile exhausts [3, 4].

The theory of atoms in molecules (AIM) and NBO analysis have become the paradigm for interpreting theoretical and experimental electron density distributions [5, 6]. Important chemical information can be retrieved from the total electron density of a molecule [7]. It proved to be appropriate to retrieve the physical and chemical significance of bond paths for very weak or supposedly repulsive interactions [8].

The present study is directed to show how molybdenum and tungsten match each other to form a stable bimetallic phosphido-bridged complex. HF and DFT methods were employed to find the accurate molecular structure of the  $\text{CpW}(\text{CO})_2(\mu\text{-PPh}_2)\text{Mo}(\text{CO})_5$  complex when the metal–metal bond forms.

Table 1

Comparison<sup>a</sup> of the molecular structure of the complex (selected bond distance and bond angle)

Parameter	$R_{(Mo1-W2)}$ , Å	$R_{(Mo1-P3)}$ , Å	$R_{(W2-P3)}$ , Å	$\angle Mo1-P3-W2$ , deg.	Av. % dev.
Experimental <sup>b</sup>	3.205	2.542	2.374	81.3	—
HF/LANL2DZ	3.459 (0.254)	2.503 (-0.039)	2.463 (0.089)	88.3 (7.0)	5.45
HF/CEP-31G	3.463 (0.258)	2.504 (-0.038)	2.470 (0.096)	88.2 (6.9)	5.52
HF/SDD	3.455 (0.250)	2.499 (-0.043)	2.471 (0.097)	88.1 (6.8)	5.49
B3LYP/LANL2DZ	3.049 (-0.156)	2.581 (0.039)	2.443 (0.069)	73.0 (-8.3)	4.88
B3LYP/CEP-31G	3.123 (-0.082)	2.577 (0.035)	2.425 (0.078)	75.5 (-5.8)	3.59
B3LYP/SDD	3.073 (-0.132)	2.573 (0.031)	2.439 (0.065)	73.9 (-7.4)	4.29
B3PW91/LANL2DZ	2.954 (-0.251)	2.546 (0.004)	2.427 (0.053)	71.2 (-10.1)	5.66
B3PW91/CEP-31G	2.980 (-0.225)	2.544 (0.002)	2.422 (0.048)	72.1 (-9.2)	5.11
B3PW91/SDD	2.967 (-0.238)	2.540 (-0.002)	2.428 (0.054)	71.7 (-9.6)	5.40
MPW1PW91/LANL2DZ	2.935 (-0.270)	2.533 (-0.009)	2.419 (0.045)	71.0 (-10.3)	5.84
MPW1PW91/CEP-31G	2.962 (-0.243)	2.533 (-0.009)	2.419 (0.045)	71.9 (-9.4)	5.35
MPW1PW91/SDD	2.949 (-0.256)	2.533 (-0.009)	2.419 (0.045)	71.5 (-9.8)	5.57
B2PLYP/LANL2DZ	3.134 (-0.071)	2.543 (0.001)	2.376 (0.002)	76.2 (-5.1)	2.15
B2PLYP/CEP-31G	3.149 (-0.056)	2.548 (0.005)	2.373 (0.001)	76.9 (-4.4)	1.85
B2PLYP/SDD	3.193 (-0.012)	2.541 (0.001)	2.378 (0.004)	77.8 (-3.5)	1.22

<sup>a</sup>The value in parentheses is the difference between the calculated parameters and the experimental data.<sup>b</sup>Ref. [1].

AIM and NBO analyses were then performed to investigate the nature of the Mo—W bond and the metal—carbonyl interactions in the binuclear  $CpW(CO)_2(\mu\text{-}PPh_2)Mo(CO)_5$  complex.

**Computational methods.** All the minimization procedures and the corresponding frequency calculations were carried out through HF [9], B3LYP [10], B3PW91 [11], MPW1PW91 [12], and B2PLYP [13] with LANL2DZ, CEP-31G, and SDD basis sets, respectively, without any geometrical constrains for the  $CpW(CO)_2(\mu\text{-}PPh_2)Mo(CO)_5$  complex. AIM analysis was performed using EXTREME (ext94b) to locate and characterize the critical points; AIM2000 was used to trace the bond paths [14]. NBO analysis was then performed with the NBO 3.1 program included in the Gaussian 09 package at the B2PLYP/GEN level of theory, SDD for W and Mo atoms, and 6-31G\* for the remain-group elements using B2PLYP/SDD optimized geometries. All HF and DFT calculations have been carried out with the Gaussian 09W program package [15].

**Results and discussion. Geometries of the  $CpW(CO)_2(\mu\text{-}PPh_2)Mo(CO)_5$  complex.** Compared with the X-ray data [1], the relevant structural parameters of the complex calculated by HF, B3LYP, B3PW91, MPW1PW91, and B2PLYP methods employing LANL2DZ, CEP-31G, and SDD basis sets, respectively, are presented in Table 1. Inspection of the data listed in Table 1 indicates that better performance in the optimized geometry of the complex could be rated in the following order: HF  $\approx$  B3PW91  $\approx$  MPW1PW91  $<$  B3LYP  $<$  B2PLYP. The results calculated by B2PLYP/SDD are closest to the experimental data for the complex, the average absolute deviation being 1.12 %. The optimized geometry obtained from B2PLYP/SDD calculations is displayed in Fig. 1. The Mo1—W2, Mo1—P3, and W2—P3 bond distances are 3.193, 2.541, and 2.378 Å, respectively. The Mo1—P3—W2 bond angle is 77.8°. The calculated Mo—W distance (3.193 Å) is consistent with the previous investigations, and falls between the values reported for  $[CpMo(CO)_2(\mu\text{-}SMe)W(CO)_5]$  (3.131 Å) and  $[(HB(pz)_3)(CO)_2W(\mu\text{-}CS)Mo(CO)_2(Ind)]$  (3.3102 Å; Ind is  $\eta\text{-}C_9H_7$ , indenyl; HB(pz)<sub>3</sub> is hydrotris(1-pyrazolyl)borate). Thus, it is appropriate to predict the physical and chemical properties of the complex based on the optimized geometry obtained at the B2PLYP/SDD level of theory.

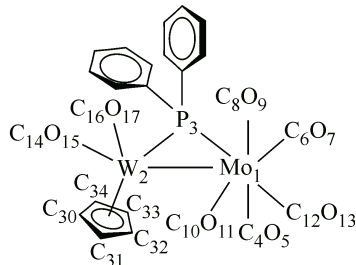


Fig. 1. Optimized geometry structure of the  $\text{CpW}(\text{CO})_2(\mu\text{-PPh}_2)\text{Mo}(\text{CO})_5$  complex and the atomic numbering system (H atoms are omitted)

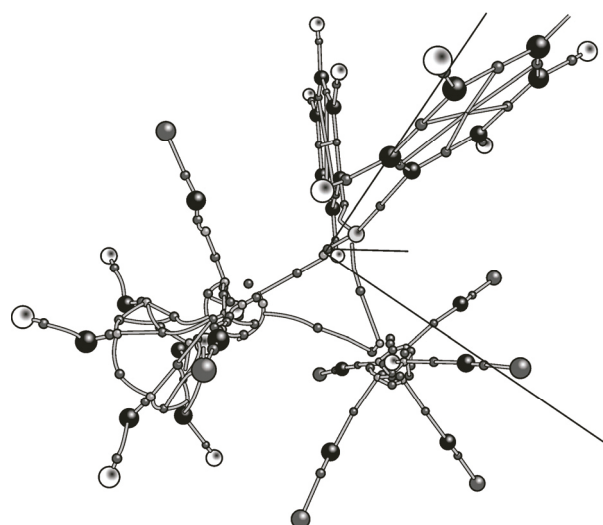


Fig. 2. BCps and bond paths in three-dimensional picture of the  $\text{CpW}(\text{CO})_2(\mu\text{-PPh}_2)\text{Mo}(\text{CO})_5$  complex

**Mo—W interaction.** A (3,−1) bond critical point (BCP) was found between Mo1 and W2, as shown in Fig. 2, which confirms the experimental claim that there is a metal—metal bond in  $\text{CpW}(\text{CO})_2(\mu\text{-PPh}_2)\text{Mo}(\text{CO})_5$ . The distances from the (3,−1) BCP to the Mo atom ( $d_1$ ) and the W atom ( $d_2$ ) are 1.616 and 1.607 Å, respectively. The bond path length (the sum of  $d_1$  and  $d_2$ ) is 3.223 Å, which is longer than the Mo—W bond (3.193 Å). It may be supposed that the Mo—W bond is bent.

The characteristics of the Mo—W (3,−1) BCP are gathered in Table 2. The  $\rho_b$  value is 0.17098 e/Å<sup>3</sup>, which is less than that for a normal C—C bond (0.18 e/Å<sup>3</sup>), suggesting that the W—Mo interaction is weak. The donor—acceptor interaction between Mo1 and W2 is taken into account as follows: (1) the negative  $\nabla^2\rho_b$  value of −0.02774 e/Å<sup>5</sup> indicates that there is a shared interaction as in a covalent bond; (2) the  $-G_b/V_b$  is 0.53941, between 0.5 and 1; (3)  $H_b$  is negative, indicating that the covalent bond is dominant; (4) the bond ellipticity is 1.29923, indicating the  $\pi$  character of the bond.

Table 2

BCP properties in the  $\text{CpW}(\text{CO})_2(\mu\text{-PPh}_2)\text{Mo}(\text{CO})_5$ <sup>a</sup> complex

Parameter	$\rho_b$ <sup>b</sup> , e/Å <sup>3</sup>	$\nabla^2\rho$ <sup>c</sup> , e/Å <sup>5</sup>	$\lambda_1$	$\lambda_2$	$\lambda_3$	$\varepsilon$ <sup>d</sup>	$G_b$ <sup>e</sup>	$V_b$ <sup>f</sup>	$H_b$ <sup>g</sup>	$-G_b/V_b$ <sup>h</sup>
(3,−1) BCP <sub>Mo1—W2</sub>	0.1710	−0.0277	−0.0870	−0.03783	0.2358	1.2992	0.1899	−0.3520	−0.1621	0.5394
(3,−1) BCP <sub>W2—C10</sub>	0.1205	−0.0276	−0.0750	−0.0363	0.2215	1.0692	0.1189	−0.2103	−0.0914	0.5655
(3,−1) BCP <sub>W2—C14</sub>	0.3151	−0.6205	−0.4066	−0.4039	3.2926	0.0066	0.9359	−1.2512	−0.3153	0.7480
(3,−1) BCP <sub>W2—C16</sub>	0.3044	−0.6053	−0.3897	−0.3729	3.1837	0.0452	0.8954	−1.1855	−0.2901	0.7553
(3,+1) RCP <sub>Mo1—W2—P3</sub>	0.1357	−0.1180	−0.0517	0.1609	0.3628	−1.3211	0.2249	−0.3317	−0.1069	0.6778
(3,+1) RCP <sub>Mo1—W2—C10</sub>	0.1151	−0.0738	−0.0332	0.1117	0.2168	−1.2972	0.1577	−0.2416	−0.0840	0.6528

<sup>a</sup> All quantities are in atomic units.

<sup>b</sup>  $\rho_b$  the charge density value at the bond (or ring) critical point.

<sup>c</sup>  $\nabla^2\rho$ , the value of the Laplacian of  $\rho_b$  at the bond (or ring) critical bond.

<sup>d</sup>  $\varepsilon$ , the bond ellipticity.

<sup>e</sup>  $G_b$ , the kinetic electron energy density.

<sup>f</sup>  $V_b$ , the potential electron energy density.

<sup>g</sup>  $H_b$ , the total energy density.

<sup>h</sup>  $-G_b/V_b$ , the ratio of the kinetic electron energy density and the potential electron energy density.

Table 3

NBO analysis at the B2PLYP/GEN//B2PLYP/SDD level of theory (selected values)<sup>a</sup>

Donor NBOs	Acceptor NBOs	$E^{(2)}$ , kcal/mol	$E(j) - E(i)$ , a.u.	$F_{(i,j)}$ , a.u.	Principal delocalization types
BD(1)Mo1—W2	BD*(1)Mo1—W2	21.10	0.69	0.101	geminal
BD(1)Mo1—W2	BD*(2)Mo1—W2	7.47	0.16	0.031	geminal
BD(1)Mo1—W2	RY*(1)W2	1.33	1.12	0.036	geminal
BD(2)Mo1—W2	RY*(2)W2	3.11	2.14	0.082	geminal
BD(2)Mo1—W2	BD*(1)Mo1—W2	16.37	2.39	0.183	geminal
BD(2)Mo1—W2	BD*(2)Mo1—W2	21.26	0.33	0.075	geminal

<sup>a</sup> BD denotes the formally occupied 2-center bonding orbital. RY\* denotes 1-center Rydberg. LP denotes a 1-center lone pair. The unstarred and starred labels denote Lewis and non-Lewis NBO, respectively. A serial number (1, 2) shows whether there is a single or double bond between the pair of atoms.

For a better understanding of the Mo—W bond and its cooperativity in the  $\text{CpW}(\text{CO})_2(\mu\text{-PPH}_2)\text{Mo}(\text{CO})_5$  complex the NBO analysis was carried out at the B2PLYP/GEN level of theory, SDD for the Mo and W atoms, and 6-31G\* for the rest of the elements using B2PLYP/SDD optimized geometries.

The donor—acceptor interaction features between Mo1 and W2 in the complex are listed in Table 3 as follows: (1) the BD(1)Mo1—W2 bond is principally delocalized on the geminal W2 1-center Rydberg, the geminal BD\*(1)Mo1—W2 anti-bond, and the geminal BD\*(2)Mo1—W2 anti-bond; (2) the BD(2) Mo1—W2 bond is principally delocalized onto the geminal W2 1-center Rydberg, the geminal BD(1)\*Mo1—W2 anti-bond, and the geminal BD(2)\*Mo1—W2 anti-bond. The primary hyperconjugative interactions  $\text{BD}(1)\text{Mo1—W2} \rightarrow \text{BD}^*(1)\text{Mo1—W2}$  and  $\text{BD}(2)\text{Mo1—W2} \rightarrow \text{BD}^*(2)\text{Mo1—W2}$  are responsible for the Mo—W interactions, having the larger charge-transfer stabilization energy ( $E^{(2)} = 21.10, 21.26$  kcal/mol, respectively) among them. This finding indicates that the formation of the Mo1—W2 interaction accompanies the dominant charge transfer interactions  $\text{BD}(1)\text{Mo1—W2} \rightarrow \text{BD}^*(1)\text{Mo1—W2}$  and  $\text{BD}(2)\text{Mo1—W2} \rightarrow \text{BD}^*(2)\text{Mo1—W2}$ . Therefore, the Mo—W dative bond in the  $\text{CpW}(\text{CO})_2(\mu\text{-PPH}_2)\text{Mo}(\text{CO})_5$  complex acts as the fifth ligand, donating two electrons to W, in addition to two COs,  $\mu\text{-PPH}_2$ , and Cp ligands coordinated to W.

**Metal—carbonyl interaction.** In addition to the metal—metal bond, the Mo—C—O angle is  $169.3^\circ$ , indicating a semi-bridging carbonyl group. The calculated W—C—O angle of  $167.4^\circ$  obtained from the B2PLYP/SDD level of theory also supports this conclusion.

A (3,+1) ring critical point, which is a point of the minimum electron density within the ring surface and a maximum on the ring line, was found among Mo1, W2, and C10, indicating that there is a three-ring interaction among Mo1, W2, and C10. The NBO analysis (Table 4) has revealed that the Mo1—C10 bond is principally delocalized onto geminal BD\*(1)Mo1—W2, geminal BD\*(2)Mo1—W2, vicinal W2 1-center Rydberg, vicinal BD\*(1)W2—P3, vicinal BD\*(1)W2—C14, vicinal BD\*(1)W2—C16.

Moreover,  $\rho_b$  of W2—C10 of  $0.12052 \text{ e}/\text{\AA}^3$  given in Table 2 is obviously much smaller than for other W2—C bonds (the  $\rho_b$  of W2—C14 and W2—C16 being  $0.31507$  and  $0.30439 \text{ e}/\text{\AA}^3$ , respectively), which indicates a weak interaction between W2 and C10. The  $\nabla^2\rho$  at BCP between W2 and C10 is negative with a small magnitude ( $-0.02756$ ), which indicates that there is a closed-shell interaction between W2 and C10. These results confirm the experimental data (IR, NMR) [1] in which  $\nu(\text{CO})$  at  $1876 \text{ cm}^{-1}$  at room temperature, and  $\delta(^{13}\text{CO})$  at  $218.69 \text{ ppm}$  at  $210 \text{ K}$  give evidence of the interaction between the W atom and the CO ligand.

The comparison of the experimental data with the calculated structural parameters demonstrates that most accurate geometry parameters are predicted by the B2PLYP/SDD level of theory among all

Table 4

*Second-order interaction energies for the complex calculated at the B2PLYP/GEN//B2PLYP/SDD level of theory (selected values)<sup>a</sup>*

Donor NBOs	Acceptor NBOs	$E^{(2)}$ , kcal/mol	$E(j) - E(i)$ , a.u.	$F(i,j)$ , a.u.	Principal delocalization types
BD(1)Mo1—C10	RY*(1)W2	3.12	3.03	0.090	vicinal
BD(1)Mo1—C10	BD*(1)Mo1—W2	115.86	2.71	0.558	geminal
BD(1)Mo1—C10	BD*(2)Mo1—W2	84.00	0.65	0.222	geminal
BD(1)Mo1—C10	BD*(1)W2—P3	67.80	2.38	0.361	vicinal
BD(1)Mo1—C10	BD*(1)W2—C14	49.82	1.91	0.361	vicinal
BD(1)Mo1—C10	BD*(1)W2—C16	59.53	2.52	0.350	vicinal

<sup>a</sup> BD denotes the formally occupied 2-center bonding orbital. RY\* denotes 1-center Rydberg. LP denotes the 1-center lone pair. The unstarred and starred labels denote Lewis and non-Lewis NBO, respectively. A serial number (1, 2) shows whether there is a single or double bond between the pair of atoms.

HF and DFT methods. Based on the B2PLYP/SDD calculations, the theory of atoms in molecules (AIM) and NBO analysis were applied as a way of quantifying the Mo—W bond and the semi-bridging carbonyl group in the  $\text{CpW}(\text{CO})_2(\mu\text{-PPh}_2)\text{Mo}(\text{CO})_5$  complex.

The presence of the Mo—W bond has been confirmed. The formation of the Mo—W interaction accompanies the dominant charge transfer interactions  $\text{BD}(1)\text{Mo1—W2} \rightarrow \text{BD}^*(1)\text{Mo1—W2}$ , and  $\text{BD}(2)\text{Mo1—W2} \rightarrow \text{BD}^*(2)\text{Mo1—W2}$ . The bond path length is 3.223 Å, which is longer than the bond distance of 3.193 Å, indicating that the Mo—W bond is not straight, but a bent one.

The presence of semi-bridging carbonyl (Mo—C—O) was demonstrated at the B2PLYP/SDD level of theory. A (3,+1) ring critical point was found among Mo1, W2, and C10, indicating a three-ring interaction among Mo1, W2, and C10. Moreover, a (3,-1) BCP was found between W2 and C10.

These findings are consistent with the experimental observations.

We are happy to thank Professor R.F.W. Bader for a copy of the EXT94B and AIM2000 programs.

#### REFERENCES

- Shyu S.G., Hsu J.Y., Lin P.J. et al. // Organometallics. – 1994. – **13**, N 5. – P. 1699 – 1710.
- Shyu S.G., Lin P.J., Wen Y.S. et al. // Organomet. Chem. – 1993. – **443**, N 1. – P. 115 – 121.
- Imler G.H., Peters G.M., Zdilla M.J. et al. // Inorg. Chem. – 2015. – **54**, N 1. – P. 273 – 279.
- Zhang Y., Roberts S.P., Bergman R.G. // Catalysis. – 2015. – **5**, N 3. – P. 1840 – 1849.
- Kucrowski I., Mitoraj M. // J. Phys. Chem. A. – 2014. – **118**, N 3. – P. 623 – 637.
- Bader R.F.W. Atoms in molecules: A Quantum Theory. – UK, Oxford: Oxford University Press, 1990.
- Sadjadi M.S., Sadeghi B., Zare K. // Spectrochim. Acta, Part A. – 2014. – **117**. – P. 413 – 421.
- Li X.H., Yin G.X., Zhang X.Z. // Chem. Phys. Lett. – 2014. – **591**. – P. 113 – 118.
- Pople J.A., Nesbet R.K. // J. Chem. Phys. – 1954. – **22**. – P. 571 – 572.
- Becke A.D. // J. Chem. Phys. – 1993. – **98**. – P. 5648 – 5652.
- Adamo C., Barone V. // J. Chem. Phys. – 1998. – **108**. – P. 664 – 675.
- Perdew J.P., Burke K., Wang Y. // Phys. Rev. B. – 1996. – **54**. – P. 16533 – 16539.
- Schwabe T., Grimme S. // Phys. Chem. Chem. Phys. – 2007. – **9**. – P. 3397 – 3406.
- Biegler-König F., Schönbohm J., Derdau R. et al. AIM2000. – Canada: McMaster University, 2002.
- Frisch M.J., Trucks G.W., Schlegel H.B. et al. Gaussian 09, Revision A. 02. – Wallingford, CT: Gaussian Inc., 2009.